

Secondary-side resonating LLC converter for reducing transformer voltage in high power applications

Hayato Nakamura, Kazuhiro Umetani, Masataka Ishihara, and Eiji Hiraki
Graduate school of natural science and technology,
Okayama University,
Okayama, Japan

Published in: 2022 International Power Electronics Conference (IPEC-Himeji 2022- ECCE Asia)

© 2022 IEEE. Personal use of this material is permitted. Permission from IEEE must be obtained for all other uses, in any current or future media, including reprinting/republishing this material for advertising or promotional purposes, creating new collective works, for resale or redistribution to servers or lists, or reuse of any copyrighted component of this work in other works.

DOI: 10.23919/IPEC-Himeji2022-ECCE53331.2022.9806826

Secondary-Side Resonating LLC Converter for Reducing Transformer Voltage in High Power Applications

Hayato Nakamura^{1*}, Kazuhiro Umetani¹, Masataka Ishihara¹, and Eiji Hiraki¹

¹ Graduate school of natural science and technology, Okayama University, Okayama, Japan

*E-mail: p19d11ul@s.okayama-u.ac.jp

Abstract—The data centers of the telecommunication infrastructure are recently consuming more electric power than before. This increasing electrical burden is requiring a small but high-power isolated power converter with a high step-down ratio. Conventionally, the LLC converter is regarded to be a promising candidate, although this converter needs vacant space for galvanic isolation due to extremely high voltage caused by the resonance in the primary side, i.e. high voltage side, of the isolation transformer, which hinders the compact implementation inside the server computers in high power design. The purpose of this paper is to propose a novel LLC converter topology to reduce this extremely high voltage by locating the LC resonator on the secondary side. The performance analysis revealed that the proposed converter exhibits a similar frequency-voltage characteristic enabling the boost and buck operation modes as well as the small rectifier conduction loss similar to the full-wave rectifier with a center-tapped transformer. The simulation confirmed the operating principles and reduction of the resonance voltage amplitude of the proposed LLC converter in comparison with the conventional LLC converter. Furthermore, the experiment also supported the operating principles, which suggests the usefulness of the proposed converter for a high voltage dc power supply system.

Keywords— *dc-dc converter, high voltage dc power supply, LLC converter.*

I. INTRODUCTION

According to the recent remarkable progress of information technology, the data centers of the telecommunication infrastructure need to process much more data than before, thus leading to increasing electrical power consumption. To cope with this increasing electric burden, the power supply system in the data centers is intensely required to be compact and efficient while accepting greater power input.

Figure 1 illustrates the typical power supply system [1]–[3] in the data center, which converts the ac power from the commercial ac power supply, as well as the uninterruptible power supply, into the low voltage dc power to feed each server computer installed in the server racks in the data center. As the server computers are recently designed to process increasing telecommunication traffic with a limited number of computers, the power consumption per server rack is also increasing. Therefore, power converters in Fig. 1 are intensely required to increase the maximum power rating without increasing the

volume. Among these power converters, the isolated dc-dc converter [4]–[10] is particularly important because it tends to occupy great space due to its isolation and high step-down functions. Therefore, the practical design of the power supply system in the server racks is intensely requiring a small but high-power isolated power converter with a high step-down ratio.

Conventionally, the LLC converter with the center-tapped secondary rectifier [6][9][10], illustrated in Fig. 2, has been regarded to be a promising converter topology for this isolated power converter. In addition to its simple circuit configuration with two magnetic devices, i.e. L_r and TR1, the LLC converter can achieve the soft-switching operation by exciting the LC resonance on the primary side with an appropriate phase angle difference between the switching gate signal and the primary winding current, which is effective to reduce the switching loss. Furthermore, the LLC converter can adjust the output voltage using the switching frequency instead of the duty cycles unlike many other power converters, which is effective to high-frequency operation because fine adjustment of the duty cycles is commonly difficult under high switching frequency over 1MHz.

Owing to these two features, the LLC converter can operate at an extremely high switching frequency, which enables the effective size reduction of the magnetic devices and capacitors. Besides, the LLC converters are commonly designed to have the center-tapped secondary rectifier [6][9][10], which is effective to reduce the conduction loss of the secondary side, which carries large ac current, and therefore beneficial in improving the efficiency, particularly in the operation at a high step-down ratio.

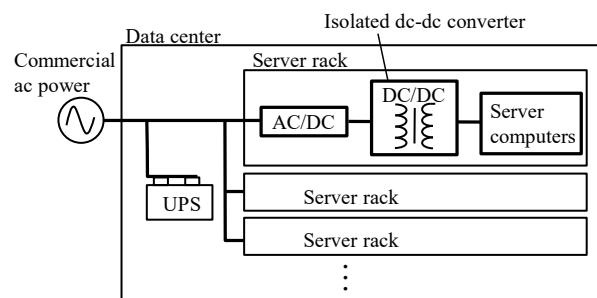


Fig. 1. Typical power supply system of data center.

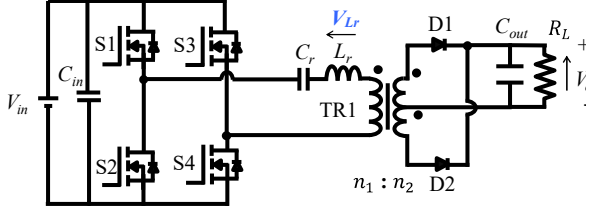


Fig. 2. Circuit schematics of conventional LLC converter.

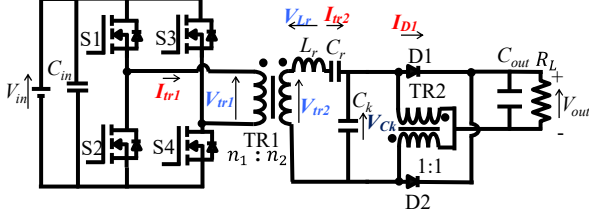


Fig. 3. Circuit schematics of proposed LLC converter.

Despite these attractive features of the LLC converter, this converter also has a drawback that hinders the high power design. The LLC converter has the LC resonator of the inductor L_r and the resonant capacitor C_r on the primary side. The resonator should be designed to have large characteristic impedance for good output voltage regulation because large characteristic impedance can cover a wide output voltage range with a small variation of the switching frequency. However, the LC resonator with large characteristic impedance will generate far larger voltage amplitude than the ac voltage that drives the resonator, particularly when the large current flows through the resonator. Therefore, inductor L_r and resonant capacitor C_r will need a large space for galvanic isolation in high power design, thus hindering the compact design of the LLC converter.

The purpose of this paper is to propose a novel resonant converter that overcomes this problem while implementing the aforementioned attractive features of the LLC converter. This proposed converter can be regarded as a variation of the LLC converter. Therefore, the proposed converter is hereafter referred to as the proposed LLC converter in contrast to the conventional LLC converter.

The following discussion comprises four sections. Section II introduces the proposed LLC converter topology and investigates its operating principles analytically. Sections III and IV present the simulation and experiment, respectively, to test the operating principle of the proposed LLC converter. Finally, section V gives the conclusions.

II. PROPOSED LLC CONVERTER

A. Circuit Topology

Figure 3 illustrates the proposed LLC converter. The proposed LLC converter incorporates the series LC resonator of L_r and C_r connected to the secondary side of the isolation transformer TR1 as well as an additional resonant capacitor C_k . Each of the two terminals of C_k is connected to a different winding of the additional

transformer TR2 and a diode that is connected to the output terminal.

The conventional LLC converter is designed to have small magnetizing inductance L_m to implement two resonant modes, i.e. the series resonance between L_r and C_r and that among L_r , L_m , and C_r , for a wide output voltage range. Meanwhile, the proposed LLC converter also implements two resonant modes without utilizing the magnetizing inductance of the isolation transformer TR1. The secondary side of the proposed LLC converter implements the series resonance between L_r and C_r and that among L_r , C_r , and C_k . By placing the resonator on the secondary side, i.e. the low voltage side, of TR1, the proposed converter can reduce the characteristic impedance of the resonator and therefore mitigate the excessive voltage excitation at L_r and C_r .

This circuit topology, which places the resonator of L_r and C_r to the secondary side of the isolation transformer, does not accept the center-tapped secondary rectifier, which is known to be effective for reducing the conduction loss at the diode. Therefore, the proposed LLC converter adopts the current doubler rectifier to output the dc electric power. The current doubler rectifier is normally made of two inductors [11]–[13]. However, this will lead to a significant increase in the volume due to the additional two magnetic devices that store magnetic energy. Therefore, in the proposed LLC converter, the current doubler rectifier is made with transformer TR2, as is utilized in [14]–[16]. This configuration of the current doubler rectifier can reduce the volume compared to the normal current doubler rectifier by reducing the number of the magnetic device and avoiding the energy storage in the device owing to adopting the transformer in replace of the two inductors.

As shown later in this section, the switching frequency was varied around the series resonant frequency of L_r and C_r . Therefore, the equivalent impedance of the secondary side circuit of the proposed LLC converter is capacitive in a wide range of the switching frequency, which may cause the hard-switching of the switching devices if TR1 has a large magnetizing inductance. For avoiding the hard-switching, TR1 should be designed to have sufficiently small but not too small magnetizing inductance to cancel the negative reactance of the secondary side circuit for maintaining the soft-switching capability in the whole operation range.

B. Operating Principles

This subsection discusses typical operation waveforms in the steady-state operation. Hereafter in this section, the following assumptions are introduced to simplify the discussion: 1 the magnetizing inductance of the transformer of the current doubler rectifier, i.e. TR2, is infinitely large; 2 the conduction loss and the switching loss is neglected in all the circuit elements except for the load resistance; 3 the magnetizing inductance of the isolation transformer TR1 is appropriately designed to achieve the soft-switching.

Figure 4 depicts the operating waveforms of the

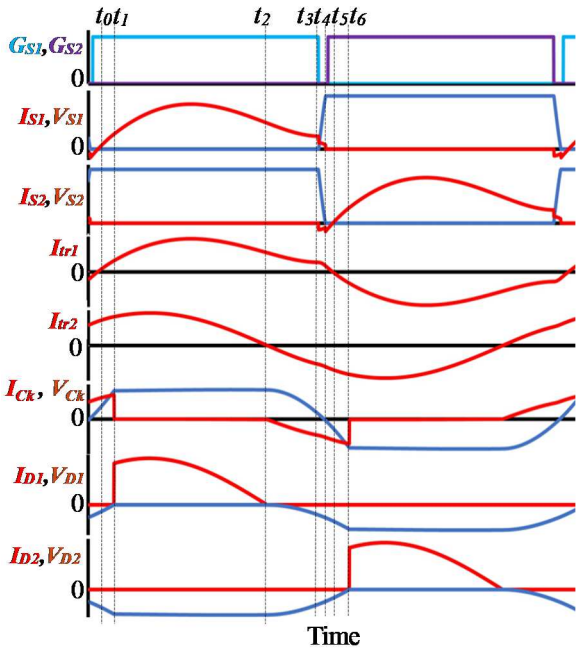


Fig. 4. Steady-state operating waveforms of proposed LLC converter.

proposed LLC converter. Similarly, as in the conventional LLC converter, the switches S1-S4 in the primary side are operated at the duty cycle of 0.5, and the leg of S1 and S2 operates with the phase shift of 180 degrees from the leg of S3 and S4. Because of the operational symmetry between the two legs, this subsection only discusses the operation in the first half period.

The operation of the half period is comprised of 6 operating modes. Figure 5 shows the current flow pattern of each operating mode. The operation of these modes is briefly summarized as follows.

Mode 1 [$t_0 < t < t_1$] (Fig. 5(a)): Switches S1 and S4 are in the on-state, thus supplying the current through the TR1 primary winding. The secondary current flows into C_k via the resonator of L_r and C_r . In this mode, the voltage of C_k is less than twice the output voltage V_{out} . Therefore, diodes D1 and D2 are reversely biased and therefore C_k is disconnected from the output.

Mode 2 [$t_1 < t < t_2$] (Fig. 5(b)): After C_k is charged to the voltage equals to twice the output voltage, the operation enters in Mode 2. In this mode, the secondary current flows through D1 via the resonator of L_r and C_r , outputting the electric power to the output smoothing capacitor C_{out} . Because transformer TR2 clips the voltage of C_k at $2V_{out}$, no current flows through C_k in this mode. Transformer TR2 induces the same amount of the current flow in its two windings. Consequently, the current flows through D1 is twice as large as the secondary current. The secondary winding current of TR1 gradually decreases after reaching the maximum current. The operation enters mode 3 after the secondary winding current crosses zero.

Mode 3 [$t_2 < t < t_3$] (Fig. 5(c)): In this mode, the secondary winding current of TR1 flows in the reverse direction, which gradually discharges C_k , whereas the primary current still flows from S1 to S4 due to the

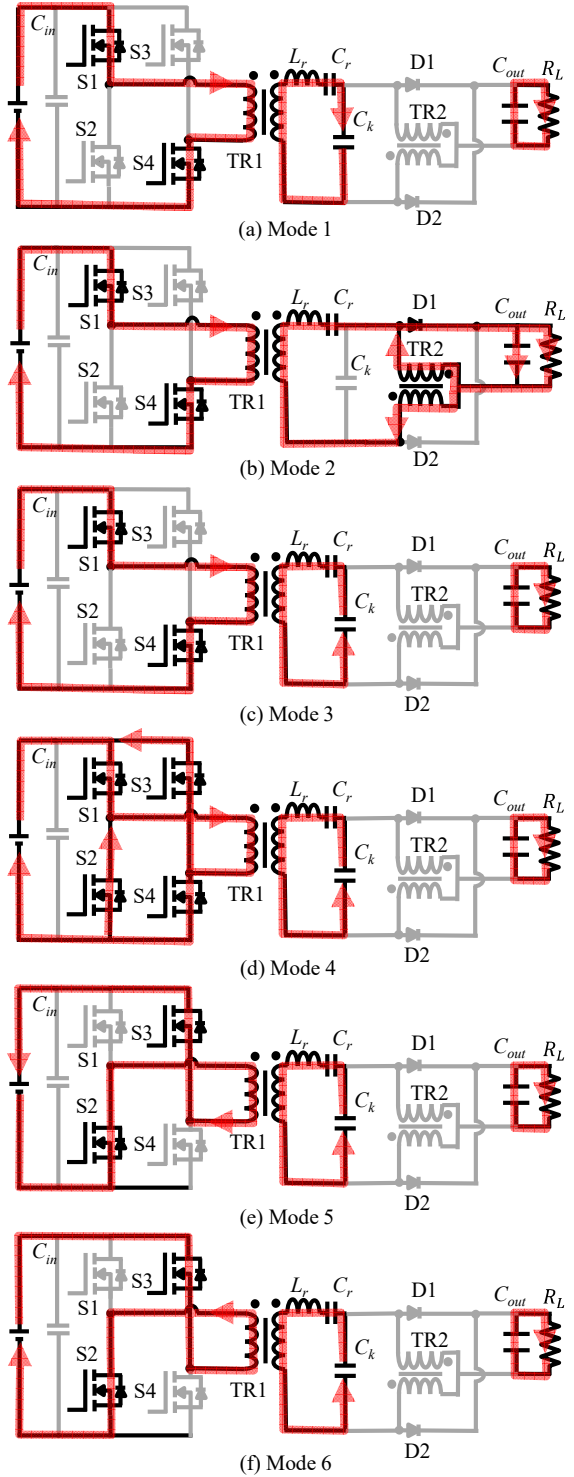


Fig. 5. Current paths in each operating mode of proposed LLC converter under steady-state operation.

magnetizing current. Because the voltage of C_k is smaller than $2V_{out}$, diode D1 is reversely biased, and therefore no current flows from the TR2 secondary windings to the output terminals.

Mode 4 [$t_3 < t < t_4$] (Fig. 5(d)): This mode corresponds to the dead time after the turn-off of S1 and S4 and before the turn-on of S2 and S3. The primary current of TR1 discharges the parasitic capacitance of these switching devices and thus achieves zero-voltage soft-switching.

The secondary current of TR1 keeps discharging C_k as in the previous mode.

Mode 5 [$t_4 < t < t_5$] (Fig. 5(e)): After the parasitic capacitance is discharged, the primary current of TR1 still keeps flowing from S2 to S3. In this state, S2 and S3 are turn-on with zero voltage transition.

Mode 6 [$t_5 < t < t_6$] (Fig. 5(f)): The primary current of TR1 changes its polarity and flows from S3 to S2, whereas the secondary current keeps discharging C_k . After this mode, the secondary current changes its polarity, entering the latter half period.

C. Dependence of Voltage Gain on Frequency

Similar to the conventional LLC converter, the voltage gain of the proposed LLC converter is dependent on the switching frequency of S1-S4 and the load resistance R_L . This subsection analyzes the voltage gain characteristics utilizing the equivalent circuit model.

The switching frequency of the proposed LLC converter varies around the resonant frequency of the series resonator of C_r and L_r . Therefore, this paper adopts the fundamental harmonic approximation (FHA) method [17]-[19] for analyzing the voltage gain. Consequently, this subsection simply regards the voltage and the current of the windings of TR1 and TR2, to be equal to the fundamental wave of the actual operating waveform. Therefore, in the FHA approximation, the primary winding of TR1 is regarded to be directly connected to the sinusoidal voltage source and the current doubler rectifier including the load, i.e. TR2, D1, D2, C_{out} , and R_L , is regarded to be an equivalent load resistance R_{AC} .

The actual voltage waveform of the TR1 primary winding is the square wave with the amplitude of V_{in} , i.e. the dc input voltage. Therefore, in this FHA analysis, the sinusoidal voltage source attached to the primary winding has the root-mean-square (RMS) value of $2\sqrt{2}V_{in}/\pi$.

The voltage waveform of C_k , i.e. the voltage of the current doubler rectifier including the load, is also a quasi-square wave with an amplitude of $2V_{out}$, where V_{out} is the dc output voltage. Therefore, the RMS voltage across the equivalent load resistance was approximated as $4\sqrt{2}V_{out}/\pi$, which indicates that this resistance consumes the electric power of $32V_{out}^2/R_{AC}\pi^2$, where R_{AC} is the equivalent load resistance. Meanwhile, the actual power consumption of the load equals V_{out}^2/R_L , where R_L is the load resistance. Consequently, by equating these two power consumption, i.e. $32V_{out}^2/R_{AC}\pi^2$ and V_{out}^2/R_L , R_{AC} was determined as $R_{AC}=32R_L/\pi^2$.

Consequently, the proposed LLC converter is reduced into the equivalent circuit shown in Fig. 6(a). Based on this equivalent circuit, a simpler equivalent circuit was derived by moving the secondary side circuit into the primary side of TR1. This multiplies the voltage and the impedance of the secondary circuit elements by n_1/n_2 and $(n_1/n_2)^2$, respectively, where n_1 and n_2 are the number of turns of the primary and secondary windings, respectively. Finally, the equivalent circuit model of the proposed LLC converter was obtained as Fig. 6(b), where L_m is the magnetizing inductance of TR1; V_{in}' , V_{out}' , R_{AC}' , L_r' , C_r' , C_k' were defined as

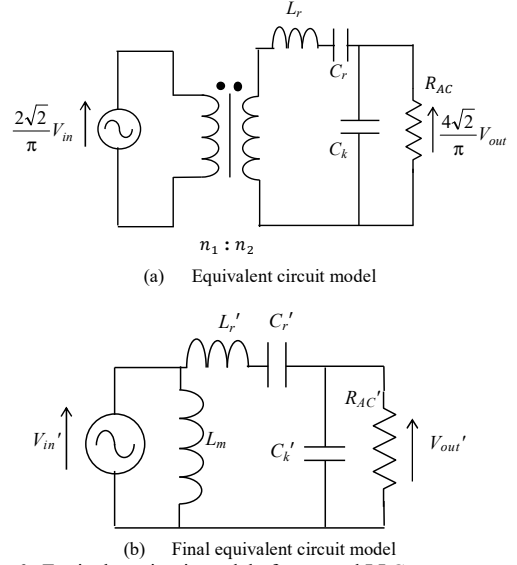


Fig. 6. Equivalent circuit model of proposed LLC converter.

$$\begin{aligned} V_{in}' &= \frac{2\sqrt{2}}{\pi} V_{out}, & V_{out}' &= \frac{4\sqrt{2}}{\pi} \frac{n_1}{n_2} V_{out}, & L_r' &= \frac{n_1^2}{n_2^2} L_r, \\ R_{AC}' &= \frac{32}{\pi^2} \frac{n_1^2}{n_2^2} R_L, & C_r' &= \frac{n_2^2}{n_1^2} C_r, & C_k' &= \frac{n_2^2}{n_1^2} C_k. \end{aligned} \quad (1)$$

By utilizing the final equivalent circuit, i.e. Fig. 6(b), the voltage gain can be analytically obtained as

$$\frac{V_{out}}{V_{in}} = \frac{n_2}{2n_1 K}. \quad (2)$$

where K is the non-dimensional number defined as

$$K = \sqrt{\left\{1 - \omega C_k' \left(\omega L_r' - \frac{1}{\omega C_r'} \right)\right\}^2 + \frac{1}{R_{AC}'} \left(\omega L_r' - \frac{1}{\omega C_r'} \right)^2}. \quad (3)$$

According to (2) and (3), the voltage gain is constant to be $n_2/2n_1$ regardless of the equivalent load resistance, if the switching frequency is identical to the resonant frequency of L_r and C_r , as is the same as the conventional LLC converter. If R_{AC}' is sufficiently greater than C_k' , the voltage gain is approximately not affected by the load resistance in a wide range of the switching frequency, which is an attractive feature different from the conventional LLC converter. In this case, the voltage gain decreases from $n_2/2n_1$, as the switching frequency decreases from this resonant frequency. Contrarily, the voltage gain increases from $n_2/2n_1$, as the switching frequency increases from this resonant frequency. Therefore, the proposed LLC converter can adjust the output voltage using the switching frequency. These features are similar to those of the conventional LLC converter, although the proposed LLC converter has the dependence of the voltage gain on the switching frequency with the inverse polarity compared with the conventional LLC converter.

TABLE I. SPECIFICATIONS OF SIMULATION AND EXPERIMENT OF PROPOSED LLC CONVERTER

| SYMBOL | Item | Value |
|-----------|--|---------------------|
| V_{in} | Input voltage | 70.3 V |
| R_L | Load resistance | 0.69 Ω |
| n_1 | Number of turns of TR1 primary winding | 8 |
| n_2 | Number of turns of TR1 secondary winding | 2 |
| f | Nominal switching frequency | 200 kHz |
| C_{in} | Input capacitance | 138 μF |
| C_{out} | Output capacitance | 50.0 μF |
| L_m | Magnetizing inductance of TR1 | 10.8 μH |
| C_r | Resonant capacitance | 0.216 μF |
| L_r | Resonant inductance | 3.08 μH |
| C_k | Capacitance | 0.200 μF |
| | TR2 turns ratio | 2:2 |

TABLE II. SPECIFICATIONS OF SIMULATION OF CONVENTIONAL LLC CONVERTER

| SYMBOL | Item | Value |
|-----------|--|--------------------|
| V_{in} | Input voltage | 70.3 V |
| R_L | Load resistance | 0.69 Ω |
| n_1 | Number of turns of TR1 primary winding | 8 |
| n_2 | Number of turns of TR1 secondary winding | 1 |
| f | Nominal switching frequency | 200 kHz |
| C_{in} | Input capacitance | 138 μF |
| C_{out} | Output capacitance | 50.0 μF |
| L_m | Magnetizing inductance of TR1 | 50.0 μH |
| C_r | Resonant capacitance | 13.5 nF |
| L_r | Resonant inductance | 49.3 μH |

III. SIMULATION

The simulation was conducted to evaluate the operating principles of the proposed LLC converter in comparison with the conventional LLC converter. The simulation models of Figs. 2 and 3 were constructed in the model space of PSIM2021a (Myway Corp.). In this simulation, a capacitor of 400 pF was attached in parallel between the drain and source terminals of each switching device because the switching devices were modeled as ideal switches. The input voltage was set at $V_{in}=70.3\text{V}$; the load resistance was set at $R_L=0.69\Omega$.

Tables I and II list the specifications of the simulation circuits. Transformers TR1 and TR2 were modeled as an ideal transformer without leakage inductance. The proposed and conventional LLC converters were designed to have the same resonant frequency of L_r and C_r . Furthermore, they were designed to cover the same output voltage range of 8.8-12.8 in the switching frequency range of 150-250kHz.

Firstly, the operating waveforms of the proposed LLC converter were evaluated under the condition that C_k was set at 0.2 μF and the switching frequency was set at 200kHz. This operating condition is expected to yield the

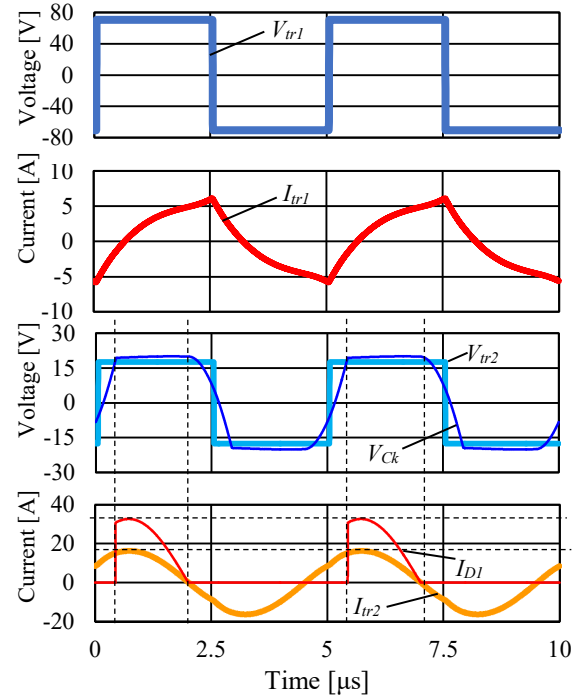


Fig. 7. Voltage and current waveforms of proposed LLC converter at $C_k=0.2\mu\text{F}$ and switching frequency of 200kHz.

output voltage of 9.9V according to the analysis of subsection II.C. Meanwhile, the simulation result of the output voltage was 9.18V.

Figure 7 shows the voltage and current waveforms of the proposed LLC converter. The relation between the voltage and current of the TR1 primary winding indicates that the switching devices that drives the primary winding can turn-on and turn-off under the zero-voltage switching, similarly to the conventional LLC converter. The TR1 secondary winding induced the square voltage waveform, which excited the sinusoidal ac current flow through L_r , which is consistent with the excitation of the LC resonance in the secondary side. This resonance current flows through C_k when the voltage of C_k is smaller than $2V_{out}$. However, the resonance current flows through D1 after the voltage of C_k reached $2V_{out}$. At this time, the current of D1 is twice as large as the resonance current due to the function of the current doubler rectifier. These features were consistent with the theory.

Next, the voltage amplitude of the series resonator of L_r and C_r was compared between the proposed and conventional LLC converters. Figure 8 shows the voltage across C_r when C_k was 0.2 μF and the switching frequency was 200kHz. This voltage was found to be the major contributor to the maximum voltage potential from the ground. As can be seen in the figure, the proposed LLC converter exhibited a great reduction of the voltage amplitude by 65.2% compared to the conventional LLC converter, enabling a compact design with easier galvanic isolation.

Finally, the switching frequency dependence of the output voltage was evaluated and compared between the proposed and conventional LLC converters. Figure 9

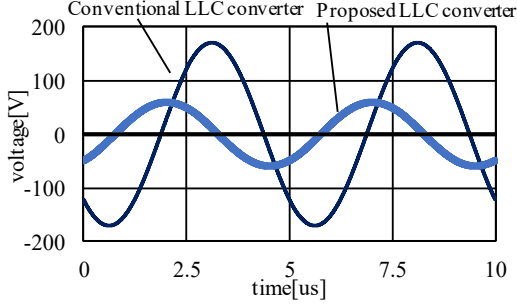


Fig. 8. Comparison of C_r voltage waveform at $C_k=0.2\mu\text{F}$ and switching frequency of 200 kHz.

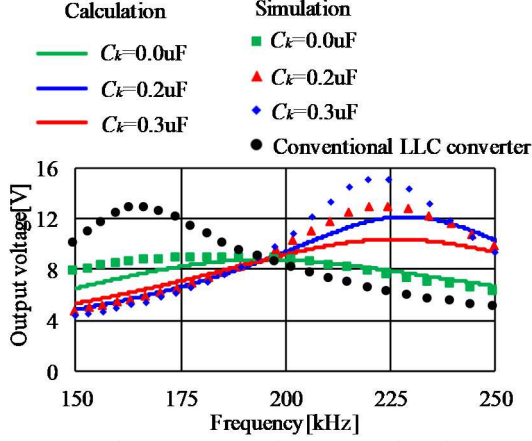


Fig. 9. Dependence of output voltage on switching frequency and C_k of proposed and conventional LLC converters.

shows the results at various values of C_k . Compared to the nominal output voltage, which is observed at the switching frequency equal to the series resonant frequency of L_r and C_r , the proposed LLC converter obtained greater output voltage at the switching frequency greater than the series resonant frequency, whereas the smaller output voltage is obtained at the frequency smaller than the series resonant frequency, as is expected from the theory. Figure 9 also shows the analytical estimation based on subsection II.C. As can be seen in the figure, the analysis well agreed with the basic features of the dependence of the output voltage on the switching frequency and C_k . Certainly, there remains a slight difference between the analysis and the simulation, which may be caused by neglecting the harmonics in the voltage and current waveforms in the analytical estimation. Nonetheless, the simulation revealed that the proposed LLC converter can have a similar output voltage range as the conventional LLC converter.

IV. EXPERIMENT

An experiment was carried out to verify the operating principles of the proposed LLC converter. This experiment evaluates the operating waveforms and the switching frequency dependence of the output voltage. Figure 10 shows the circuit diagram of the experimental prototype of the proposed LLC converter. The proposed converter directly connects the TR1 primary winding to the inverter and therefore ideally needs the inverter control to eliminate magnetic dc bias in the transformer. However, the experimental prototype instead added the capacitor

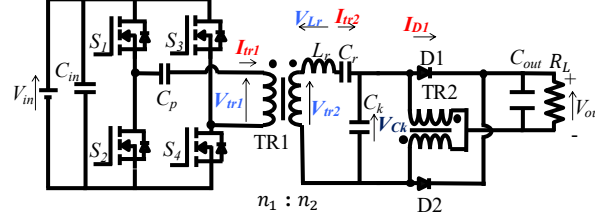


Fig. 10. Circuit diagram of experimental prototype of proposed LLC converter.

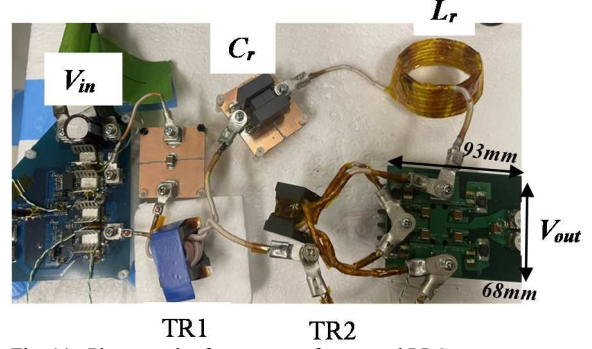


Fig. 11. Photograph of prototype of proposed LLC converter.

TABLE III. PARAMETER SPECIFIC TO EXPERIMENT

| Circuit elements | Value |
|---|--------------------|
| Magnetizing inductance of TR2 | 15.6 μH |
| Leakage inductance of TR2 | 66.3nH, 71.4 nH |
| Capacitor attached in series of TR1 primary winding | 10.0 μF |

TABLE IV. CIRCUIT ELEMENTS USED IN PROTOTYPE OF PROPOSED LLC CONVERTER

| Circuit elements | Model No. |
|--|------------------|
| Gate drivers for S1-S4 | SI823H8AD-IS3 |
| Gate resistor connected between the gate driver and MOSFET S1-S4 | 5 Ω |
| MOSFET S1-S4 | IPT60R040S7XTMA1 |
| Diode(Two diodes are connected in parallel to form D1 and D2, respectively.) | V30100S-E3/4W |
| Transformer TR1 core material | B65879B0000R087 |
| Transformer TR2 core material | B65879B0000R087 |

with sufficiently large capacitance in series to the primary winding to prohibit the dc current flow through the primary winding for simple experimental setting without the control.

Figure 11 shows the photograph of the prototype of the proposed LLC converter, constructed for this experiment. The basic specifications of the proposed LLC converter were the same as shown in Table I. However, unlike the simulation, TR1 and TR2 of the prototype contain the leakage inductance and TR2 also has the magnetizing inductance. The specifications of parameters only for the experiment were listed in Table III.

Table IV shows the circuit element list utilized in the experimental prototype. Transformers TR1 and TR2 were made of the ferrite core with the windings of the Litz wire. Meanwhile, the resonant inductor L_r was made as a coreless solenoid of Litz wire, for simple construction. The film capacitors were employed for the resonant capacitor

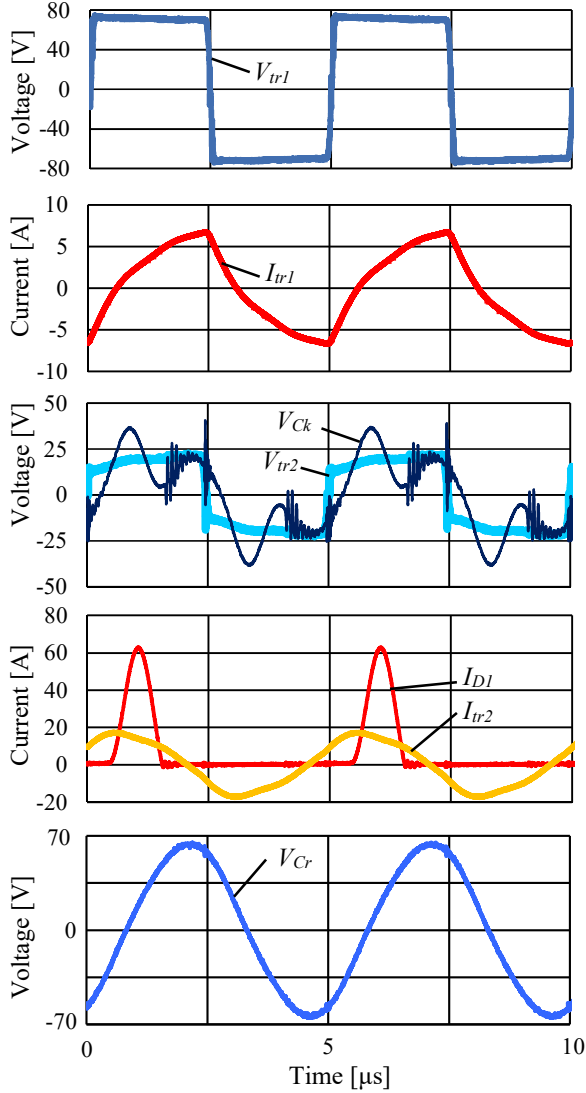


Fig. 12. Experimental results of the operating waveforms.

C_r due to its large voltage amplitude, whereas the ceramic capacitors were employed for the other capacitors.

In this experiment, the input voltage of the prototype was set at 70.3V; the load resistance was set at 0.69Ω . The experimental results were compared with the simulation results based on the same circuit model as the previous section for evaluating the consistency between the experiment and the simulation. (The circuit parameters and operating conditions of the simulation were set to be the same as the experiment.)

Figure 12 shows the experimental results of the operating waveforms. The experiment exhibited similar operating waveforms consistent with the analytically predicted operation in section II, indicating the appropriateness of the operating principles. The voltage and current of the primary windings indicate the zero-voltage turn-on and turn-off of the switching devices. Certainly, a slight difference was found in the voltage and current waveforms in the rectifier, particularly in the voltage of C_k and the current of D1. This discrepancy is caused by the parasitic resonance between C_k and the leakage inductance of TR2. The simulation in the previous section did not consider the leakage inductance of TR1 and

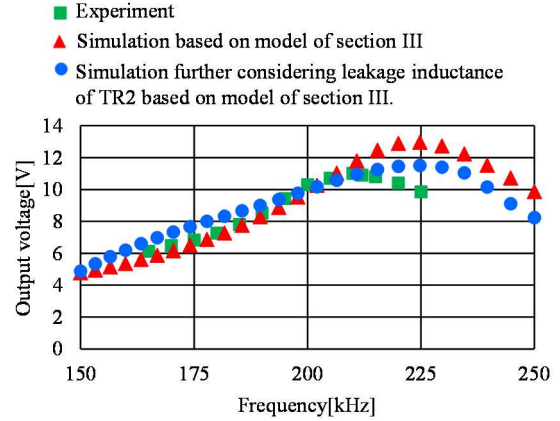


Fig. 13. Experimental result of output voltage characteristic in comparison with simulation.

TR2, which may have resulted in this discrepancy between the experiment and the simulation.

Figure 13 shows the experimental output voltage characteristics with various values of C_k in comparison with the simulation. The experiment exhibit similar switching frequency dependence to the simulation, although the maximum output voltage deteriorated. The reason for this deterioration is not clear in this paper. However, the probable cause may be the leakage inductance of the transformers and the power loss of the circuit elements including the magnetic devices, which was not considered in the simulation. In fact, the simulation further considering the leakage inductance of TR2 yielded closer voltage gain characteristic than that without the leakage inductance, i.e. the simulation model identical to section III. This implies that the transformer of the rectifier needs to reduce the leakage inductance for the practical implementation of the proposed LLC converter. Consequently, despite the small discrepancy from the simulation, the fundamental features were successfully verified by the experiment.

V. CONCLUSIONS

Recently, the power supply systems for the telecommunication infrastructure require a small but high-power isolated power converter with a high step-down ratio. The LLC converter has been regarded to be a promising candidate, although the excessively high voltage induction of the LC resonator placed on the primary side hindered practical implementation for the power supply system. To overcome this difficulty, this paper proposed a novel LLC converter, which has an LC resonator on the secondary side. Similarly to the conventional LLC converter, the proposed LLC converter is operated at the switching frequency around the resonant frequency of the LC resonator and can control the output voltage by adjusting the switching frequency. Furthermore, the switching devices of the proposed LLC converter can operate under the soft-switching operation. The simulation and the experiment successfully validated the basic operating principles, although the design optimization and the performance comparison including the efficiency will be investigated in future researches.

REFERENCES

- [1] S. Mondal and E. Keisling, "Efficient data center design using novel modular DC UPS, server power supply with DC voltage and modular CDU cooling," in Proc. IEEE Intl. Conf. Power Electron., Drives Energy Syst. (PEDES), 2012, pp. 1-6.
- [2] S. Qi, W. Sun and Y. Wu, "Comparative analysis on different architectures of power supply system for data center and telecom center," in Proc. IEEE Intl. Telecommunications Energy Conf. (INTELEC), 2017, pp. 26-29.
- [3] B. R. Shrestha, U. Tamrakar, T. M. Hansen, B. P. Bhattarai, S. James and R. Tonkoski, "Efficiency and reliability analyses of AC and 380 V DC distribution in data centers," IEEE Access, vol. 6, pp. 63305-63315, 2018.
- [4] R. Simanjorang, H. Yamaguchi, H. Ohashi, T. Takeda, M. Yamazaki and H. Murai, "A high output power density 400/400V isolated DC/DC converter with hybrid pair of SJ-MOSFET and SiC-SBD for power supply of data center," in Proc. IEEE Appl. Power Electron. Conf. Expo. (APEC), 2010, pp. 648-653.
- [5] P. Das, M. Pahlevaninezhad and A. Kumar Singh, "A novel load adaptive ZVS auxiliary circuit for PWM three-level DC-DC converters," IEEE Trans. Power Electron., vol. 30, no. 4, pp. 2108-2126, April 2015.
- [6] M. Mu and F. C. Lee, "Design and optimization of a 380-12 V high-frequency, high-current LLC converter with GaN devices and planar matrix transformers," IEEE J. Emerg. Sel. Top. Power Electron., vol. 4, no. 3, pp. 854-862, Sept. 2016.
- [7] M. Ahmed, C. Fei, F. C. Lee and Qiang Li, "High-efficiency high-power-density 48/1V sigma converter voltage regulator module", in Proc. IEEE Appl. Power Electron. Conf. Expo., pp. 2207-2212, 2017.
- [8] E. Candan, P. S. Shenoy and R. C. N. Pilawa-Podgurski, "A series-stacked power delivery architecture with isolated differential power conversion for data centers," IEEE Trans. Power Electron., vol. 31, no. 5, pp. 3690-3703, May 2016.
- [9] C. Fei, F. C. Lee and Q. Li, "High-efficiency high-power-density LLC converter with an integrated planar matrix transformer for high-output current applications," IEEE Trans Ind. Electron., vol. 64, no. 11, pp. 9072-9082, Nov. 2017.
- [10] M. H. Ahmed, F. C. Lee and Q. Li, "Two-stage 48-V VRM with intermediate bus voltage optimization for data centers," IEEE J. Emerg. Sel. Top. Power Electron., vol. 9, no. 1, pp. 702-715, Feb. 2021.
- [11] Xinbo Ruan, Bin Li, Jiangang Wang and Jinzhong Li, "Zero-voltage-switching PWM three-level converter with current-doubler-rectifier," IEEE Trans. Power Electron., vol. 19, no. 6, pp. 1523-1532, Nov. 2004.
- [12] P. Alou, J. A. Oliver, O. Garcia, R. Prieto and J. A. Cobos, "Comparison of current doubler rectifier and center tapped rectifier for low voltage applications," in Proc. IEEE Appl. Power Electron. Conf. Expo., 2006, pp. 1-7.
- [13] Hong Mao, Liangbin Yao, Songquan Deng, O. Abdel-Rahman, Jun Liu and I. Batarseh, "Inductor current sharing of current doubler rectifier in isolated DC-DC converters," in Proc. IEEE Appl. Power Electron. Conf. Expo., 2006, pp. 1-6.
- [14] J. Y. Shin, H. W. Kim, K. Y. Cho, S. S. Hwang, S. K. Chung and G. B. Chung, "Analysis of LLC resonant converter with current-doubler rectification circuit", in Proc. Power Electron. Motion Ctrl. Conf. Expo. (PEMC), Sept. 2014, pp. 162-167.
- [15] D. H. Lee, J. Y. Shin, S. S. Hwang, B. K. Lim and H. W. Kim, "Analysis of the efficiency characteristics of an LLC resonant converter having a current doubler rectification circuit", in Proc. Intl Conf. Elect. Mach. Syst. (ICEMS), Oct 2015, pp. 480-484.
- [16] S. Nigsch, M. Schlenk and K. Schenk, "Detailed analysis of a current-doubler rectifier for an LLC resonant converter with high output current", in Proc. IEEE Appl. Power Electron. Conf. Expo. (APEC), pp. 1748-1754, 2017.
- [17] Yusuke Murakami, Terukazu Sato, Kimihiro Nishijima, Takashi Nabeshima, "Small signal analysis of LLC current resonant converters using equivalent source model", in Proc. Annu. Conf. IEEE Ind. Electron. Soc., pp. 1417-1422, 2016.
- [18] H. Huang, "FHA-based voltage gain function with harmonic compensation for LLC resonant converter", in Proc. IEEE Appl. Power Electron. Conf., pp. 1770-1777, 2010.
- [19] G. Ivensky, S. Bronshtein, and A. Abramovitz, "Approximate analysis of resonant LLC DC-DC converter," IEEE Trans. Power Electron., vol. 26, no 11, pp. 3274-3284, 2011.